

Segregation characteristics of irregular binaries in gas solid fluidized beds – An ANN approach

A. Sahoo* and G. K. Roy

Department of Chemical Engineering, National Institute of Technology, Rourkela-769008, Orissa, India

*Author to whom correspondence should be addressed. Tel:+91-661-2463258 (R), 2462258 (O),
Fax: +91-661-2472926, E-Mail: abantisahoo@gmail.com and asahu@nitrkl.ac.in

Abstract Binary mixtures of irregular materials of different particle sizes and / or particle densities are fluidized in a 15cm diameter column with a perforated plate distributor. An attempt has been made in this work to determine the segregation characteristics of jetsam particles for both the homogeneous and heterogeneous binary mixtures in terms of segregation distance by correlating it to the various system parameters, viz. initial static bed height, height of a layer of particles above the bottom grid, superficial gas velocity and average particle size and / or particle densities of the mixture through the dimensional analysis. Correlation on the basis of *Artificial Neural Network* approach has also been developed with the above system parameters thereby authenticating the development of correlation by the former approach. The calculated values of the segregation distance obtained for both the homogeneous and heterogeneous binary mixtures from both the types of fluidized beds (i.e. under the static bed condition and the fluidized bed condition) have also been compared with each other.

Keywords gas-solid fluidization, segregation distance, static bed condition, fluidized bed condition, irregular binaries and artificial neural network

1. Introduction

Segregation or de-mixing is a major problem especially encountered in gas-solid fluidization of homogeneous and heterogeneous mixtures. Segregation can even be a problem in mixers, whereby over-mixing can actually lead to segregation. More commonly, the major segregation problems occur after mixing. This may occur during discharge or transport and handling. The problem mainly occurs when there are differences in the mobility of the particles caused by different sizes, densities and/or shapes. The higher the mobility difference, the greater is the segregation. This is a prime problem with food mixes that contain bigger dried particulates mixed with powders, which may easily segregate during

transport and handling after mixing. As a result, there is a need for measuring segregation tendency to give an index of the problem, a greater understanding of the segregation mechanism, and procedure for trying to overcome these short-comings. Ideal particulate systems consisting of monosized particles of equal densities seldom occur in gas-solid fluidized bed applications, where mostly mixtures of different sizes and/or densities are encountered. In these non-ideal systems, mixing and segregation can occur within specific operation conditions (Wu and Baeyens, 1998).

Previous studies on gas solid fluidization of multi-component solid mixture (Tanimoto et al., 1981) have shown that particle segregation takes place in particular in the vertical direction of a bed when there is an appreciable density/size difference between particles. Under certain operating conditions, the segregation pattern can easily be detected by examining the vertical concentration profile of one of the components of the mixture. A bed may be fluidized in the sense that all the particles are fully supported by the gas, but may still be segregated in the sense that the local bed composition does not correspond with the overall average. Segregation is likely to occur when there is substantial difference in the drag/unit weight ratio between different particles. Particles having a higher drag/unit weight ratio migrate to the distributor (Wu and Baeyens, 1998).

2. Literature

Gibilaro and Rowe (1974) proposed a mathematical model by formulating conservation equation for jetsam particles relative to the bulk particles due to the rise of one single gas bubble in a fluidized bed. Tanimoto et al. (1981) observed that the jetsam particles descend relative to the bulk particles. Thus they defined the segregation distance as the relative distance of the jetsam to the bulk particles due to the rise of one single gas bubble entrained with the particles, and measured the same by taking the difference between the two drift lines. They also observed that more segregation took place in a three-dimensional bed compared to a two-dimensional bed.

The distance thus obtained would be equal to the mean settling distance if the region wherein drift occurred corresponded exactly with the cross-sectional area of the bubble (in fact, significant drift occurs up to a distance of three bubble radii from the centre of the rising bubble). They defined the dimensionless average segregation distance (Y_s) reduced over

the bubble cross sectional area. The empirical dimensionless segregation distance related to the properties of the jetsam and flotsam was proposed by Tanimoto et al. (1981) as follows:

$$Y_s = 0.6 \times \left(\frac{\rho_j}{\rho_b} \right) \times \left(\frac{d_j}{d_b} \right)^{0.33} \cdot \dots\dots\dots (1)$$

Hoffmann et al. (1993) modified the above model further as

$$Y_s = 0.8 \times \left(\frac{\rho_j}{\rho_{bulk}} \right) \times \left(\frac{d_j}{d_{bulk}} \right)^{0.33} - 0.8 \cdot \dots\dots\dots (2)$$

Dechsiri et al. (2001) introduced a concentration term of the flotsam to the above equation and presented the expression for the dimensionless segregation distance as

$$Y_s = 0.8 \times \left[\frac{\rho_j (d_j)^{0.33}}{C_f (\rho_f (d_f)^{0.33}) + (1 - C_f) (\rho_j (d_j)^{0.33})} - 1 \right] \cdot \dots\dots\dots (3)$$

In the present work the experimental segregation distance values have been calculated using the above equation for both static and fluidized bed conditions.

3. Experimental

The experimental set up as shown in Fig.1 consists of a 15cm x100cm fluidizer, a rotameter, a manometer, a compressor, a distributor and a vacuum system. Air was used as the fluidizing medium. A binary mixture of irregular particles of two different sizes and / or densities with a specific mixture composition was fluidized in the fluidizer at a particular superficial gas velocity. When steady state prevailed, samples were drawn from different heights of the bed through the side ports for analyzing the jetsam concentration at different layers in fluidizing condition (This is referred to as fluidized bed condition). Again the bed was made static after fluidizing for some time by shutting off the air supply; then the bed was divided into different layers. Each layer of 2cm was drawn by vacuum for analyzing the jetsam concentration (This is referred to as static bed condition). This process was repeated by varying the various system parameters, viz. size and -/- or density of the bed materials, composition of the binaries, initial static bed height, superficial velocity of the fluidizing

medium and the height of the layer of particles above the grid, which are listed as the scope of the experiment in Table 1-A and 1-B.

4. Development of Correlations

4.1 Dimensionless Analysis Approach:-

No direct method is available to measure or calculate the segregation distance for a system. In the present case, Eq. 3 was used to calculate the segregation distance of the jetsam particles in any layer - by using the values of experimentally measured jetsam concentration at that position. Attempt has been made to correlate the segregation distance thus obtained with the various system parameters for both the homogeneous and heterogeneous binaries. Plots of the experimental segregation distance against the system parameters for both the static and the fluidized bed conditions and for both the types of binaries are shown in Fig. 2-A, 2-B and Fig. 3-A, 3-B respectively. The final correlations are as follows:

(A) Homogeneous Binaries

For static bed condition:

$$Y_s = 0.051 \left[\left(\frac{d_j}{d_f} \times \frac{d_m}{d_f} \right)^{1.134} \left(\frac{H_s}{D_c} \right)^{0.031} \left(\frac{H_b}{D_c} \right)^{0.016} \left(\frac{U_o}{U_{mf}} \right)^{-0.015} \right] \cdot \dots (4)$$

For fluidized bed condition:

$$Y_s = 0.052 \left[\left(\frac{d_j}{d_f} \times \frac{d_m}{d_f} \right)^{1.151} \left(\frac{H_s}{D_c} \right)^{0.002} \left(\frac{H_b}{D_c} \right)^{0.001} \left(\frac{U_o}{U_{mf}} \right)^{-0.001} \right] \cdot \dots (5)$$

(B) Heterogeneous Binaries

For static bed condition:

$$Y_s = 0.178 \times \left[\left(\frac{\rho_f}{\rho_j} \times \frac{\rho_m}{\rho_j} \right)^{-1.207} \left(\frac{H_s}{D_c} \right)^{0.040} \left(\frac{H_b}{D_c} \right)^{0.010} \left(\frac{U_o}{U_{mf}} \right)^{-0.008} \right] \cdot \dots (6)$$

For fluidized bed condition:

$$Y_s = 0.186 \times \left[\left(\frac{\rho_f}{\rho_j} \times \frac{\rho_m}{\rho_j} \right)^{-1.190} \left(\frac{H_s}{D_c} \right)^{0.012} \left(\frac{H_b}{D_c} \right)^{0.011} \left(\frac{U_o}{U_{mf}} \right)^{-0.001} \right]. \quad \dots\dots (7)$$

4.2 Artificial neural network approach:

An ANN-based model has been defined in literature as a computing system made up of a number of simple and highly interconnected processing elements, which processes information by its dynamic state response to external inputs. The back propagation network is the most well known and widely used among the current types of neural network systems. The same has been used in the present study to develop the model in the above mentioned form, where different values for the coefficient and exponents have been found (Sahoo and Roy, 2007). An attempt has been made to develop an ANN-model in the Supervised Learning framework. A three layered feed forward Neural Network is considered for this problem. The network is trained with a given number of data sets, where each set consists of four system parameters and the corresponding experimental value of the segregation distance (Y_s). The ANN-parameters are listed in Table 2. The network structure together with the learning rate was varied to obtain an optimum structure (shown in Fig. 4) with a view to minimizing the mean square error at the output.

These data sets were obtained from the experimental observations. The data were scaled down and then the network was exposed to these scaled data sets. The network weights were updated using the Back Propagation algorithm. The considered sigmoidal activation function is expressed as follows:

$$f(x) = 2.0 \times \left(\frac{1}{1 + e^{-\lambda \cdot x}} - 0.5 \right). \quad \dots\dots\dots (8)$$

where, λ is the slope parameter which determines the slopes of the activation function.

The training data sets were impressed repeatedly for maximum of 30,000 no. of epochs till the mean square error is below a pre-specified threshold. The network with the weights obtained from the training is now exposed to the prediction data set and thereby 98 sets of output data were computed.

The final coefficient and exponents of correlation computed by the ANN-approach were determined by averaging the 97 sets of output data components and then multiplying with the respective scaling factor. The final correlations thus developed are as given below.

(A) Homogeneous Binaries

For static bed condition:

$$Y_s = 0.05 \times \left[\left(\frac{d_j}{d_f} \times \frac{d_m}{d_f} \right)^{1.155} \left(\frac{H_s}{D_c} \right)^{0.032} \left(\frac{H_b}{D_c} \right)^{0.012} \left(\frac{U_o}{U_{mf}} \right)^{-0.015} \right]. \quad \dots\dots\dots (9)$$

For fluidized bed condition:

$$Y_s = 0.052 \times \left[\left(\frac{d_j}{d_f} \times \frac{d_m}{d_f} \right)^{1.172} \left(\frac{H_s}{D_c} \right)^{0.002} \left(\frac{H_b}{D_c} \right)^{0.001} \left(\frac{U_o}{U_{mf}} \right)^{-0.003} \right]. \quad \dots\dots\dots (10)$$

(B) Heterogeneous Binaries

For static bed condition:

$$Y_s = 0.178 \times \left[\left(\frac{\rho_f}{\rho_j} \times \frac{\rho_m}{\rho_j} \right)^{-1.206} \left(\frac{H_s}{D_c} \right)^{0.041} \left(\frac{H_b}{D_c} \right)^{0.010} \left(\frac{U_o}{U_{mf}} \right)^{-0.008} \right]. \quad \dots\dots\dots (11)$$

For fluidized bed condition:

$$Y_s = 0.173 \times \left[\left(\frac{\rho_f}{\rho_j} \times \frac{\rho_m}{\rho_j} \right)^{-1.297} \left(\frac{H_s}{D_c} \right)^{0.015} \left(\frac{H_b}{D_c} \right)^{0.012} \left(\frac{U_o}{U_{mf}} \right)^{-0.003} \right]. \quad \dots\dots\dots (12)$$

5. Results and Discussion

The mean square errors for learning of the data for both types of fluidized beds are shown in Fig. 5-A and 5-B (sample plots for both types of mixtures) respectively. It is observed that the mean square error values obtained for 100 numbers of epochs in each case remain constant up to 30,000 cycles (maximum number of epochs) for both types of beds and both types of irregular binaries thus implying the proper training of data. The values of segregation distance calculated with Eq. (4) & Eq. (9) and Eq.(5) & (10) for the static and the fluidized bed conditions by DA-approach & ANN-approach respectively are compared with the experimental values in Fig. 6 and Fig. 7 respectively. A comparison has also been made for

both types of beds in Fig. 8 where good agreement has been found for both types of binaries in most of the cases. The mean and the standard deviation for the two methods viz. for DA-approach and ANN-approach for both types of binaries are listed in Table 3. It is observed that the effects of other system parameters in comparison with the particle size/density on segregation distance are less. Even though the particle size/density play the dominating role in the segregation of the binary mixtures of the particles, the effects of other parameters on the segregation characteristic of binary mixture cannot be ignored.

6. Conclusion

The models developed by the ANN approach were tested against experimental values and were also compared with the model developed by the dimensional analysis approach for both static and fluidized bed conditions for both types of binaries. The results obtained were found to be well within reasonable limits, implying thereby its applicability to a wide range of process conditions. Thus the correlations developed by the dimensional analysis approach have been completely authenticated by the ANN-models for different types of beds and different types of particle mixtures. Under identical conditions, the calculated values of the segregation distance have been found to be higher for the fluidized bed condition than for the static bed condition.

More work is also required to include particle/particle interference and the response of the mixing and segregation parameters to the local jetsam concentration, which changes the local U_{mf} . When this is achieved the maximum concentration no longer has to be imposed in the numerical evaluation. This would also automatically make the model account for defluidization of the bottom part of the bed for fluidization velocities below the U_{mf} of the jetsam.

Therefore the developed experimental models can be used widely for analyzing the segregation characteristics of both heterogeneous and homogeneous binaries over a good range of the operating parameters. Thus it can be concluded that the segregation tendency irrespective of the type of binaries (homogeneous or heterogeneous) is promoted in the fluidizing condition thereby providing a method for its potential application in solid-solid separation based on density/size difference.

Nomenclature

C	:	Concentration of particles at any height in the bed	
D_C	:	Diameter of the column,	m
d	:	Average particle size,	m
H_b	:	Height of particle's layer in the bed from the distributor,	m
H_s	:	Initial static bed height,	m
K	:	Coefficient of the correlation	
U	:	Superficial velocity of the fluidizing medium,	m/s
Y_s	:	Segregation distance, dimensionless	
ρ	:	Density,	kg/m ³

Subscripts:

o	:	operating condition
mf	:	minimum fluidizing condition
j	:	jetsam
f	:	flotsam
b	:	bulk
m	:	average/mean for the mixture
p	:	particle

Abbreviations:

ANN : Artificial Neural Network

D A : Dimensional analysis

dia_ratio : combined system variable, $\left(\frac{d_j}{d_f} \times \frac{d_m}{d_f} \right)$

Dm : $d_j \times d_m$

Df : $d_f \times d_f$

dens_factor : combined system variable, $\left(\frac{\rho_f}{\rho_j} \times \frac{\rho_m}{\rho_j} \right)$

ρ_{r1} : $\frac{\rho_f}{\rho_j}$

$$\rho_{r2} \quad : \quad \frac{\rho_m}{\rho_j}$$

References

1. Dechsiri, C., Bosman, J. C., Dehling, H. G., Hoffmann, A. C. and Hui, G.; Proceedings of International Congress on Particle Technology, (PARTEC-2001), March-2001; Numberg.
2. Gibilaro, L. G. and Rowe, P. N. (1974). A model for a segregating gas fluidized bed. Chem. Eng. Sci., 29, 1403 -1422.
3. Hoffman, A.C., Janssen, L. P. B. M. and Prins, J. (1993). Particle segregation in fluidized binary mixtures. Chemical Engineering Science, 48, 1583 -1592.
4. Sahoo, A. and Roy, G. K. (2007). Artificial Neural Network approach to segregation characteristic of homogeneous mixtures in promoted gas-solid fluidized beds. Powder Technology, 171 54-62.
5. Tanimoto, H., Chiba, S., Chiba, T. and Koboyasi, H. (1981). Jetsam descent induced by a single bubble passage in three-dimensional gas-fluidized beds. Journal of Chemical Engineering of Japan, 14, 273-276.
6. Wu, S. Y. and Baeyens, J. (1998). Segregation by size difference in gas fluidized beds. Powder Technology, 98 139-150.

Table Caption

Table 1 Scope of experiment

(A) For homogeneous binary mixtures							
Sl. No.	Bed material	Size of jetsam $d \times 10^3, m$	Size of flotsam $d \times 10^3, m$	Mass ratio of jetsam to flotsam in mixture	Average particle size of the mixture $d \times 10^3, m$	Initial static bed height $H_s, \times 10^2, m$	Heights of layers for the withdrawal of samples, $H_b \times 10^2, m$
1	Dolomite	1.015	0.725	25:75	0.7975	12	2,4,6,8,10,12
2	Dolomite	1.015	0.725	25:75	0.7975	14	2,4,6,8,10,12,14,
3	Dolomite	1.015	0.725	25:75	0.7975	16	2,4,6,8,10,12,14,16
4	Dolomite	1.015	0.725	25:75	0.7975	20	2,4,6,8,10,12,14,16,18,20
5	Dolomite	1.015	0.725	10:90	0.754	20	2,4,6,8,10,12,14,16,18,20
6	Dolomite	1.015	0.725	40:60	0.841	20	2,4,6,8,10,12,14,16,18,20
7	Dolomite	1.015	0.725	50:50	0.870	20	2,4,6,8,10,12,14,16,18,20
8	Dolomite	1.29	0.725	25:75	1.0075	20	2,4,6,8,10,12,14,16,18,20
9	Dolomite	1.44	0.725	25:75	1.0825	20	2,4,6,8,10,12,14,16,18,20
10	Dolomite	1.7	0.725	25:75	1.2125	20	2,4,6,8,10,12,14,16,18,20
(B) For heterogeneous binary mixtures							
Sl. No.	Bed material	Density of flotsam $\rho_p, kg/m^3$	Density of jetsam $\rho_p, kg/m^3$	Mass ratio of jetsam to flotsam in mixture	Average particle density of the mixture $\rho_m, kg/m^3$	Initial static bed height $H_s \times 10^2, m$	Heights of layers for the withdrawal of samples, $H_b \times 10^2, m$
1	Coal & Iron	1430	4760	25:75	2262.5	20	2,4,6,8,10,12,14,16,18,20
2	Refr.brick & Iron	2550	4760	25:75	3102.5	20	2,4,6,8,10,12,14,16,18,20
3	Latrite & Iron	3390	4760	25:75	3732.5	20	2,4,6,8,10,12,14,16,18,20
4	Dolomite & Iron	2940	4760	25:75	3395	20	2,4,6,8,10,12,14,16,18,20
5	Dolomite & Iron	2940	4760	10:90	3122	20	2,4,6,8,10,12,14,16,18,20
6	Dolomite & Iron	2940	4760	40:60	3668	20	2,4,6,8,10,12,14,16,18,20
7	Dolomite & Iron	2940	4760	50:50	3850	20	2,4,6,8,10,12,14,16,18,20
8	Dolomite & Iron	2940	4760	25:75	3395	16	2,4,6,8,10,12,14,16
9	Dolomite & Iron	2940	4760	25:75	3395	18	2,4,6,8,10,12,14,16,18
10	Dolomite & Iron	2940	4760	25:75	3395	22	2,4,6,8,10,12,14,16,18,20

Table 2 ANN Parameters

ANN-Parameters	Static condition	Fluidized condition
Type	Three layered, Back Error Propagation	Three layered, Back Error Propagation
Slope parameter (λ)	0.95	0.95
Learning _ rate (α)	0.001	0.01
Number of training	93	92
Number of testing	97	97
Maximum cycles /	30000	30000
Input nodes	5	5
No. of hidden nodes	4	4
No. of output nodes	6	6

Table 3 Deviation of calculated values of segregation distance from experimental values

	STATIC BED CONDITION		FLUIDIZED BED CONDITION	
	D.A.-approach	ANN-approach	D.A.-approach	ANN-approach
Homogeneous Binaries				
Standard deviation, %	6.5414	6.1882	5.8788	5.5482
Mean deviation, %	5.2917	5.5242	4.8104	5.5137
Heterogeneous Binaries				
Standard deviation, %	7.269	7.2549	6.958	7.908
Mean deviation, %	4.9042	4.9516	4.436	5.589

Figure Caption

- Fig. 1 :** Experimental set-up.
- Fig. 2 :** Correlation plot for segregation distance against system parameters for homogeneous binaries.
- Fig. 3 :** Correlation plot for segregation distance against system parameters for heterogeneous binaries.
- Fig. 4 :** Optimum structure for Artificial Neural Network.
- Fig. 5 :** Mean square error plot against no. of epochs for training of data by ANN-approach.
- Fig. 6 :** Comparison of experimental and calculated values of segregation distance (by both DA and ANN approaches) for homogeneous binaries.
- Fig. 7 :** Comparison of experimental and calculated values of segregation distance (by both DA and ANN approaches) for heterogeneous binaries.
- Fig. 8 :** Comparison of calculated values of segregation distance for the static bed and the fluidized bed by DA-approach.

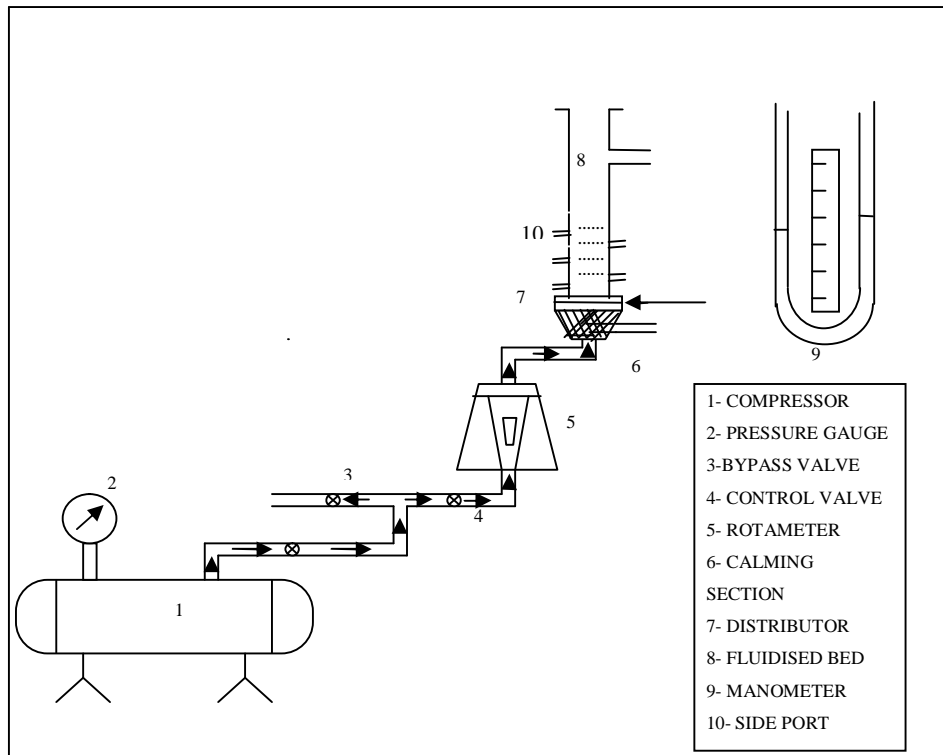
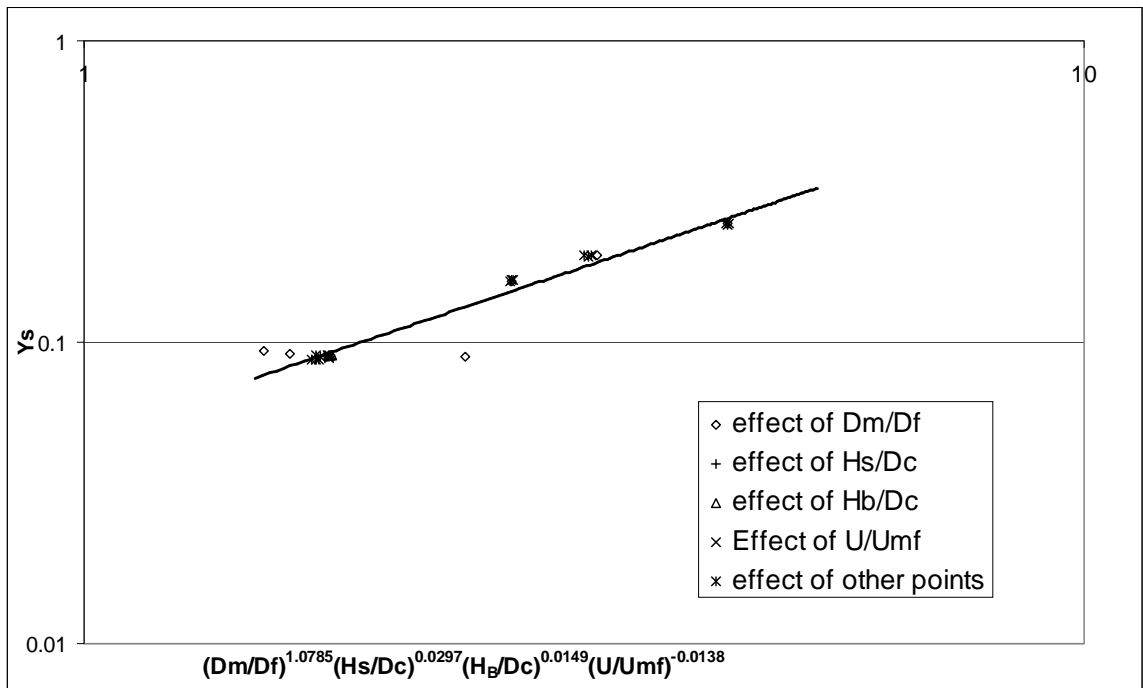


Fig. 1 Experimental set-up

A. STATIC BED



B. FLUIDIZED BED

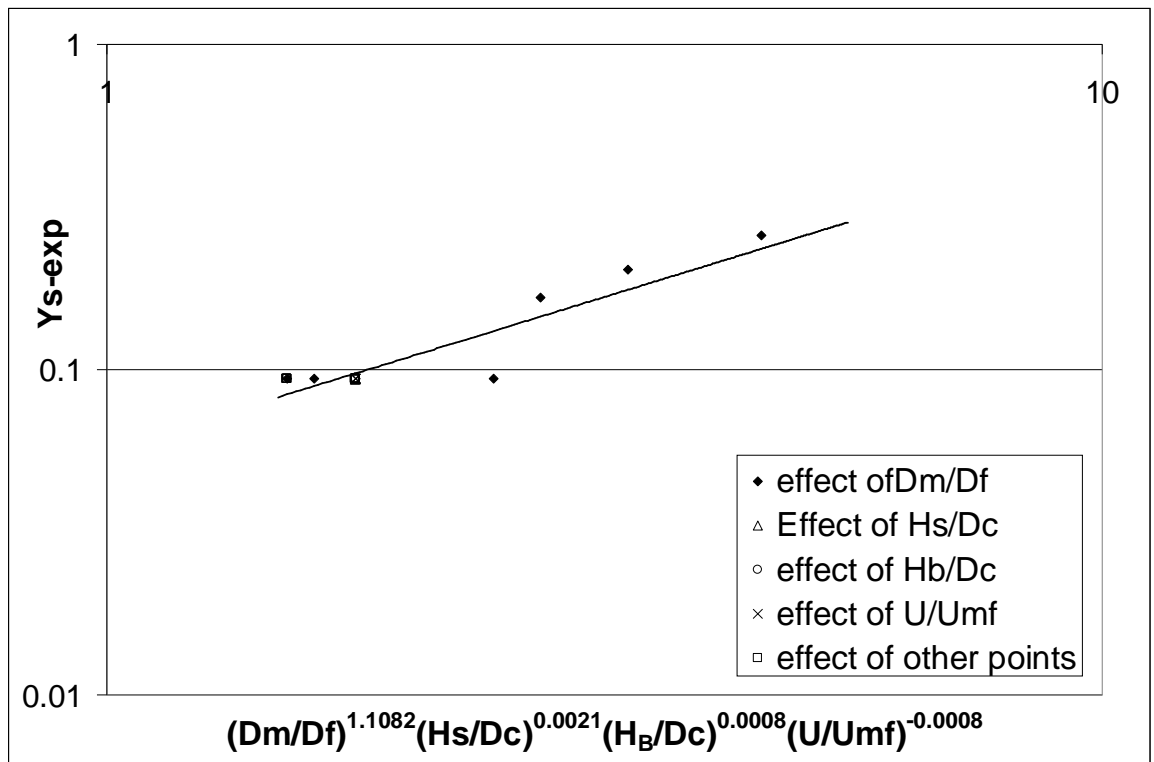
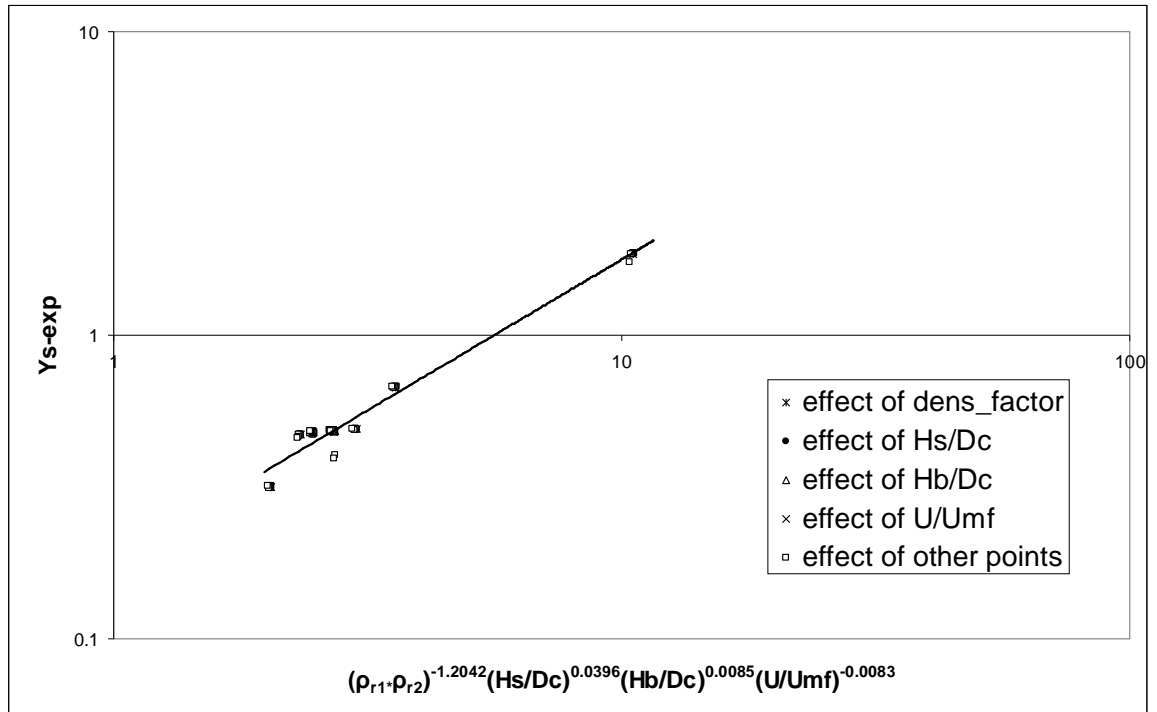


Fig. 2 Correlation plot for segregation distance against system parameters for Homogeneous Binaries.

A. STATIC BED



B. FLUIDIZED BED

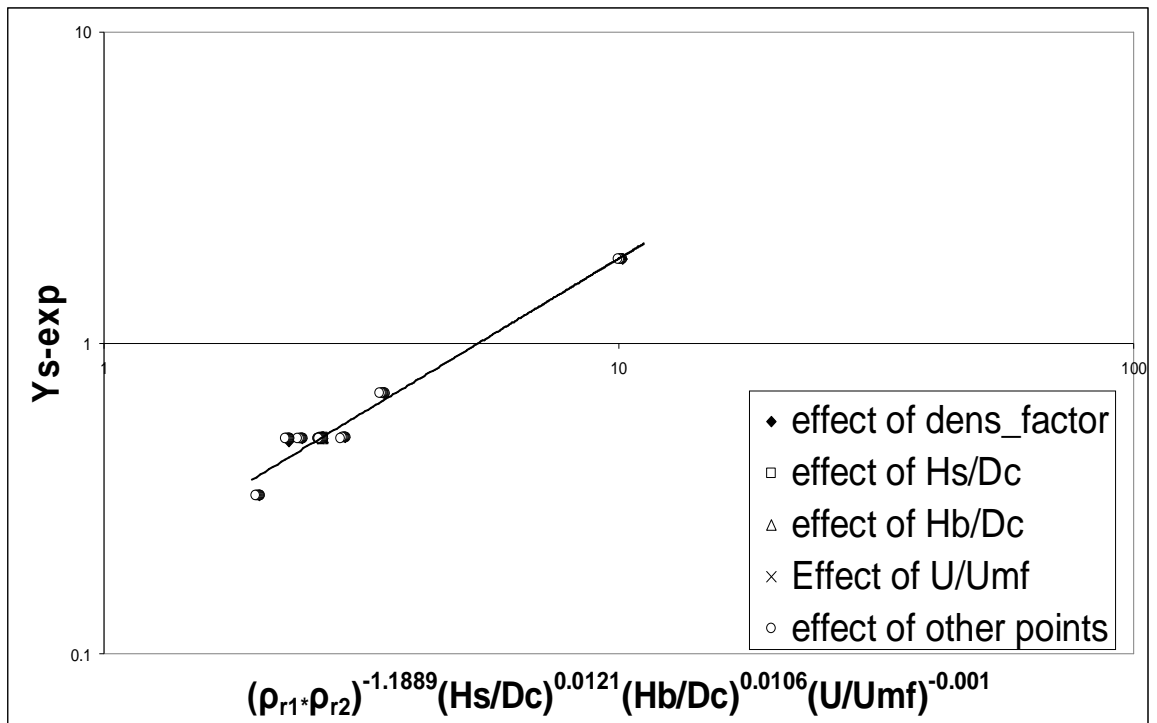


Fig. 3 Correlation plot for segregation distance against system parameters for Heterogeneous Binaries

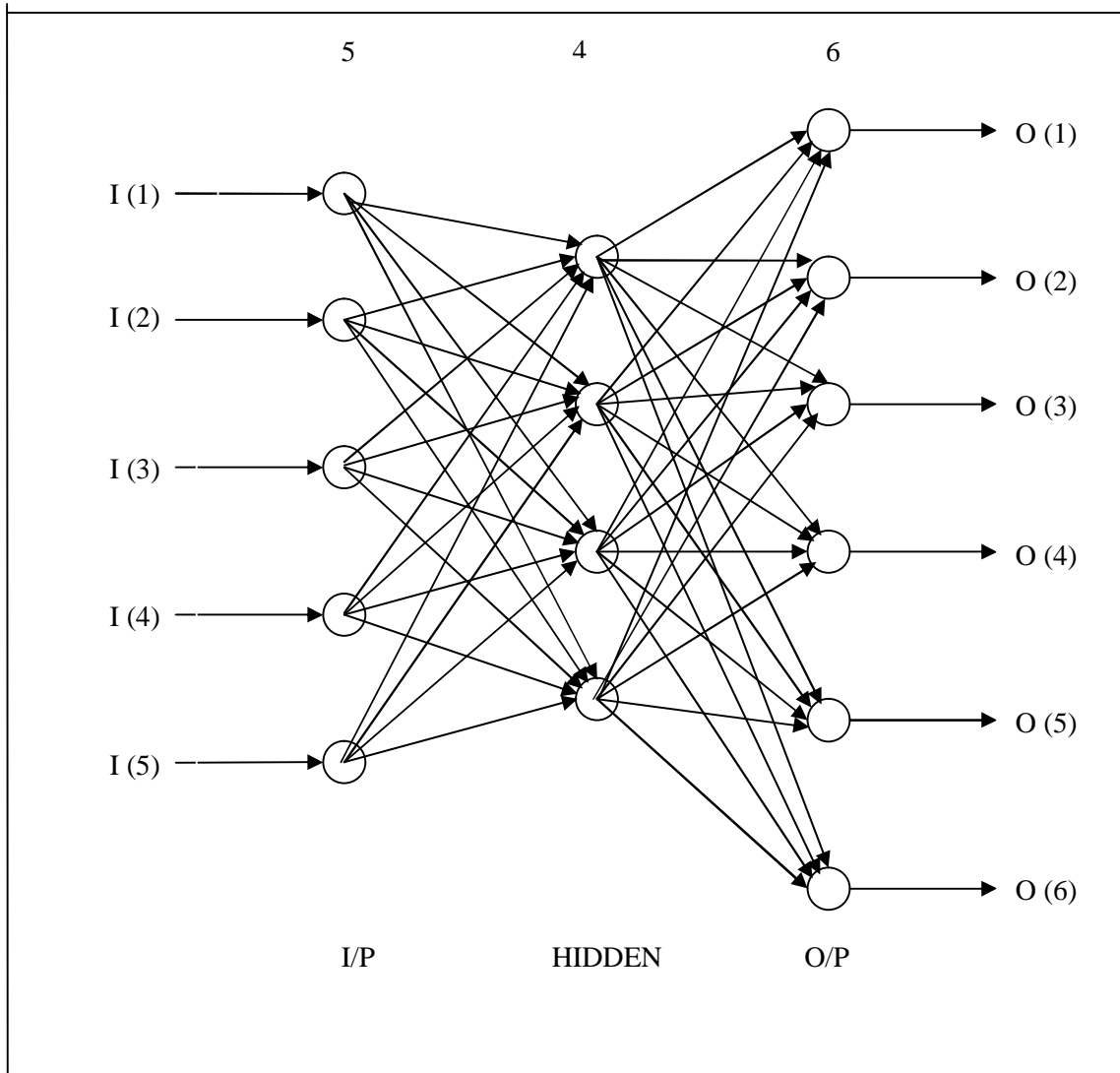
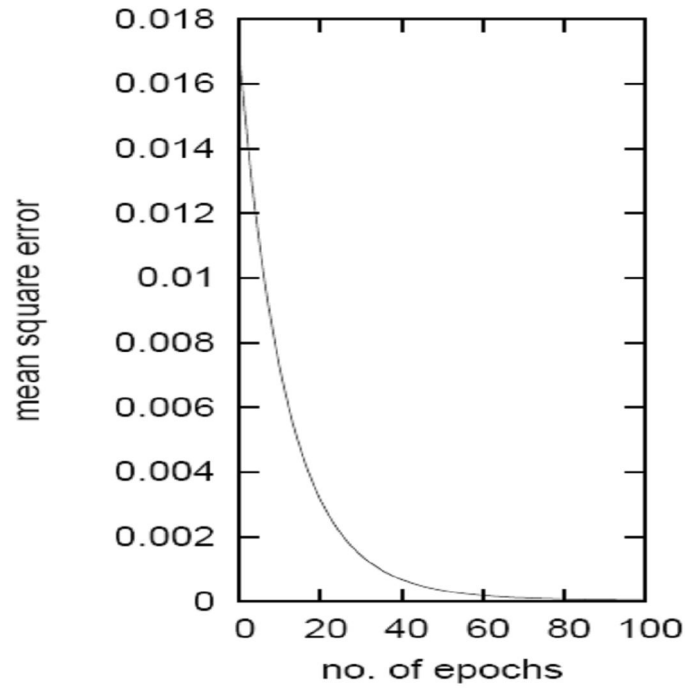


Fig. 4 Optimum structure for Artificial Neural Network.

A. STATIC BED-HOMOGENEOUS MIXTURE



B. FLUIDIZED BED-HETEROGENEOUS MIXTURE

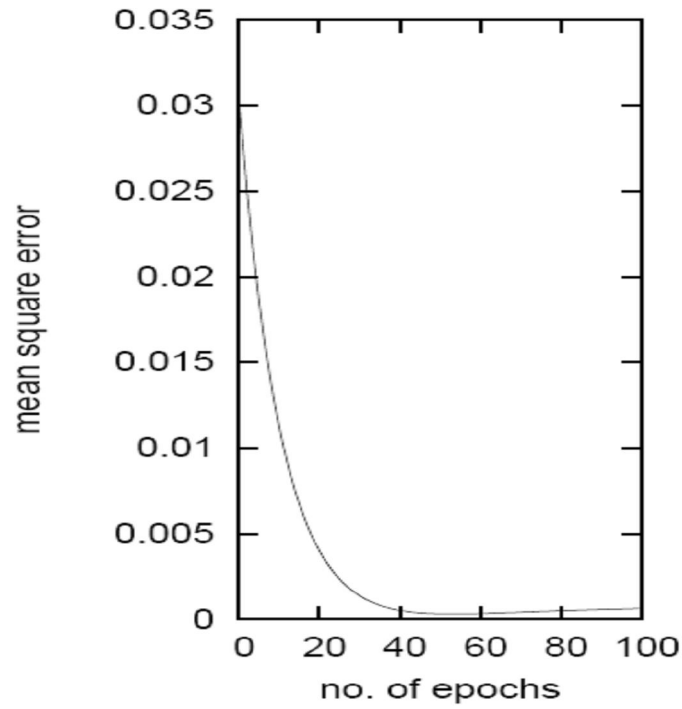
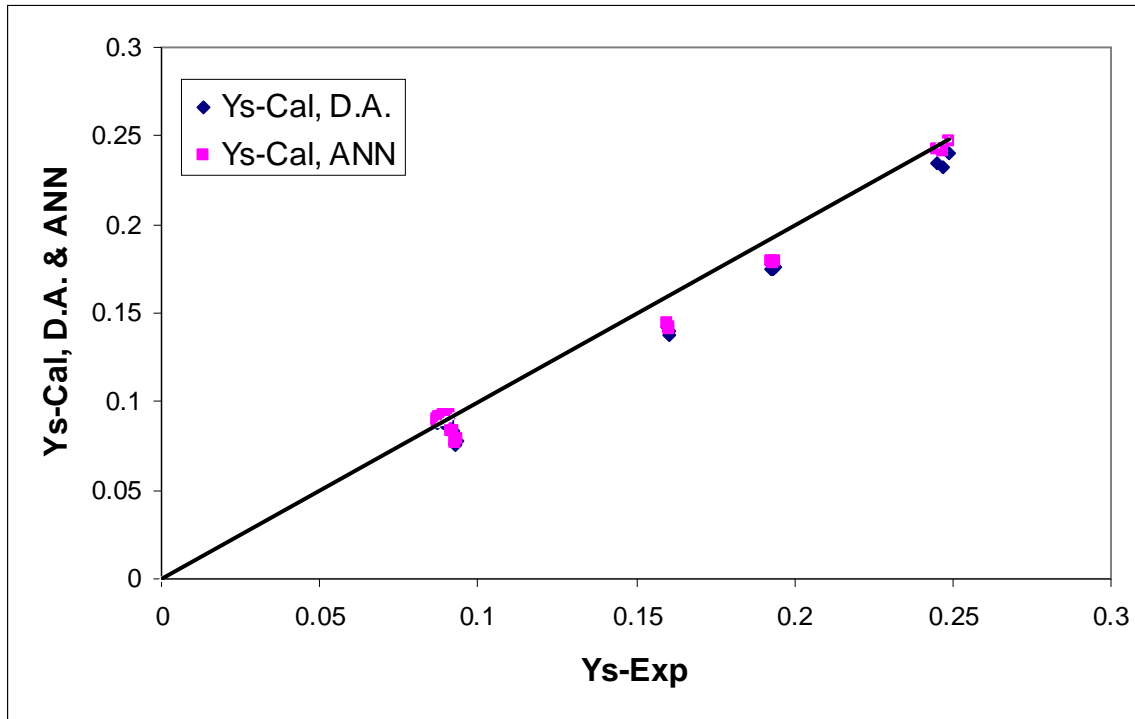


Fig. 5 Mean square error plot against no. of epochs for training of data by ANN-approach for Binaries

A. STATIC BED



B. FLUIDIZED BED

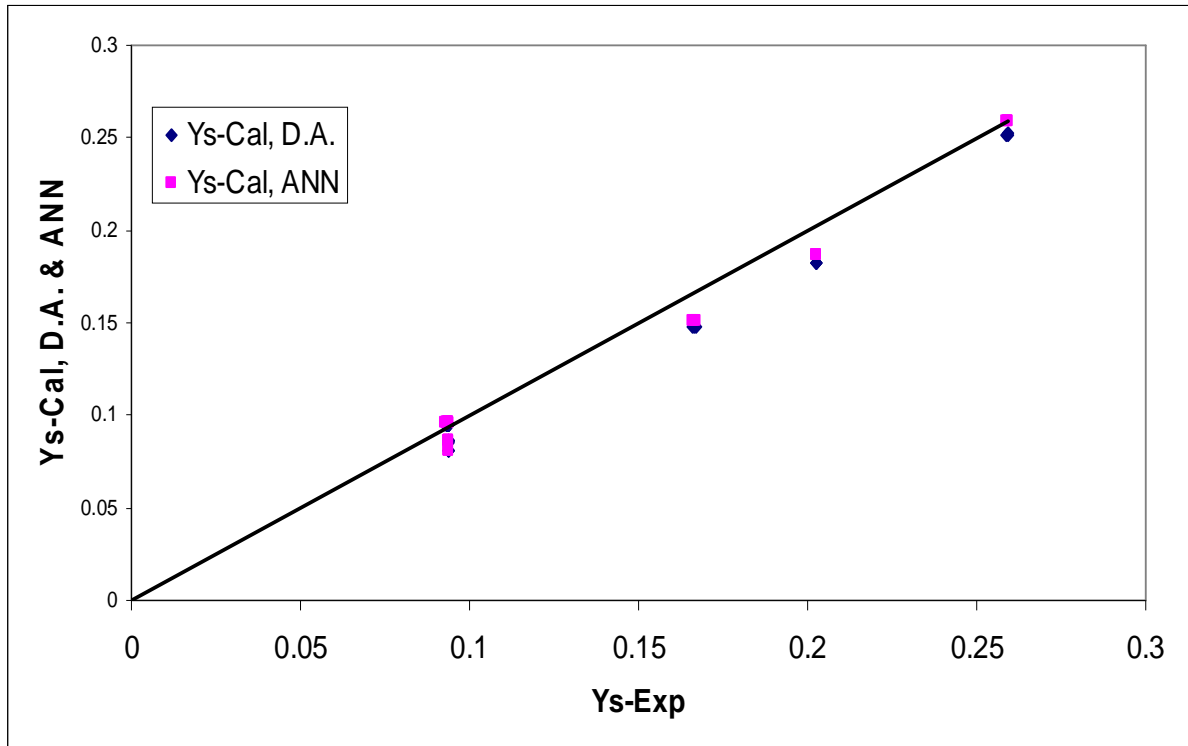
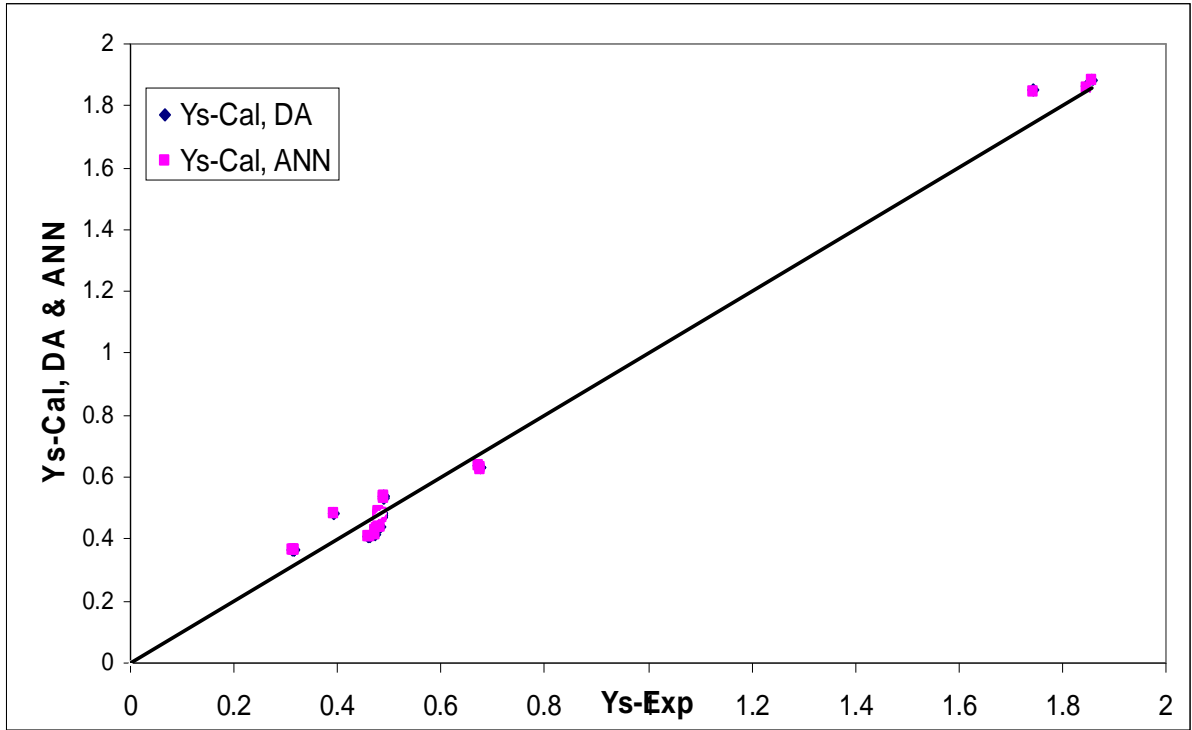


Fig. 6 Comparison of experimental and calculated values of segregation distance (by both D.A. and ANN approaches) for Homogeneous Binaries

A. STATIC BED



B. FLUIDIZED BED

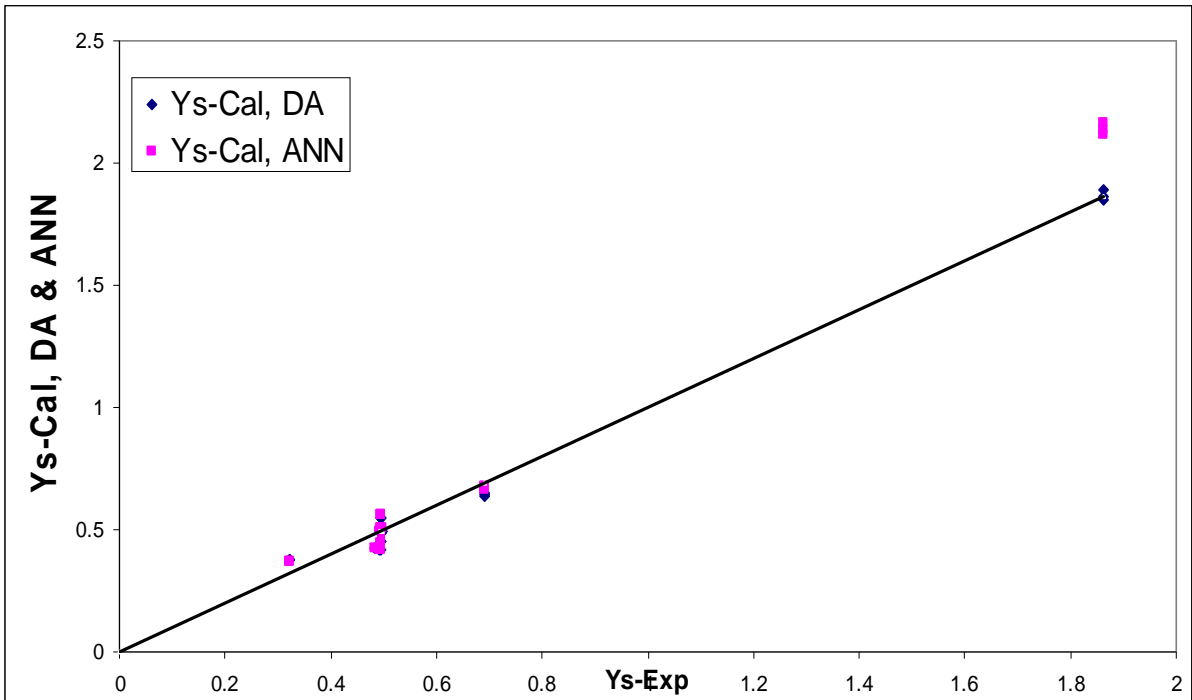
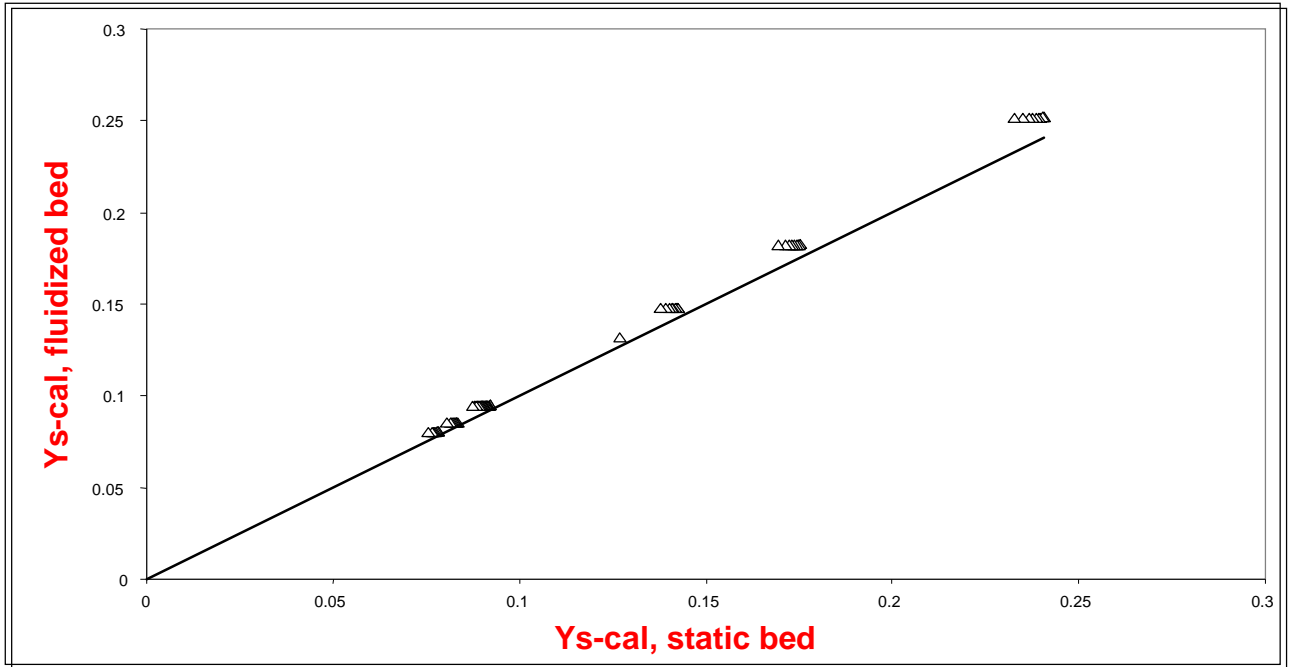


Fig. 7 Comparison of experimental and calculated values of segregation distance (by both D.A. and ANN approaches) for Heterogeneous Binaries

A. HOMOGENEOUS BINARIES



B. HETEROGENEOUS BINARIES

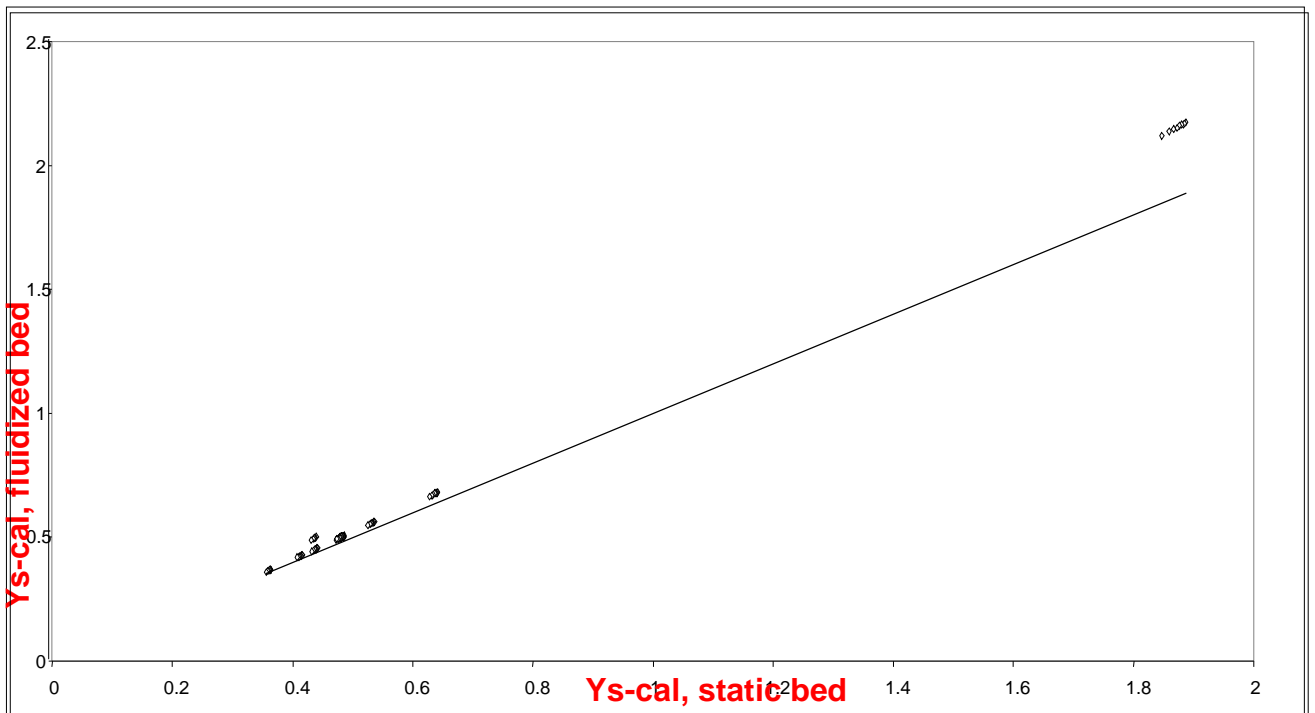


Fig. 8 Comparison of calculated values of segregation distance for the static bed and the fluidized bed by DA-approach

